

# Passivity Based Control of Four-Switch Buck-Boost DC-DC Converter without Operation Mode Detection

Hasan Komurcugil<sup>1</sup>, Sertac Bayhan<sup>2,3</sup>, Naki Guler<sup>4</sup> and Ramon Guzman<sup>5</sup>

<sup>1</sup> Department of Computer Engineering, Eastern Mediterranean University, Famagusta, Via Mersin 10, Turkey

<sup>2</sup> Qatar Environment and Energy Research Institute, Hamad Bin Khalifa University, Doha, Qatar

<sup>3</sup> Department of Electrical-Electronic Engineering, Technology Faculty, Gazi University, Ankara, Turkey

<sup>4</sup> Electrical and Energy Department, Technical Science Vocational School, Gazi University, Ankara, Turkey

<sup>5</sup> Technical University of Catalonia, Spain

[hasan.komurcugil@emu.edu.tr](mailto:hasan.komurcugil@emu.edu.tr), [sbayhan@hbku.edu.qa](mailto:sbayhan@hbku.edu.qa), [gulern@gazi.edu.tr](mailto:gulern@gazi.edu.tr), [ramon.guzman@upc.edu](mailto:ramon.guzman@upc.edu)

**Abstract**—This paper presents a passivity-based control approach for four-switch buck-boost (FSBB) DC-DC converters. The state variables are selected as the inductor current and the capacitor voltage errors. The passivity based control is formulated that targets to drive the inductor current and capacitor voltage to their reference values. The reference of the inductor current is produced by a proportional-integral controller that operates on the capacitor voltage error. Two control input equations are defined for buck and boost operations due to the fact that FSBB converter contains separate switches for buck and boost stages. As a consequence of controlling each stage by the dedicated control input, the passivity based control method eliminates the need for using a mode detection algorithm. The validity and superiority of the proposed approach has been studied by Matlab/Simulink simulations under load step, reference voltage step and operation mode variations for buck and boost modes. The results reveal that the proposed control approach can regulate the output voltage under all cases.

**Index Terms**—Four switch buck-boost converter, duty cycle, voltage regulation, current control, passivity based control.

## I. INTRODUCTION

Due to the significant advantages such as wide operating voltage range, buck/boost operation capability and bidirectional power flow, the four-switch buck-boost (FSBB) DC-DC converters are extensively preferred in many areas such as telecommunication systems [1], photovoltaic power generation [2], LED applications [3], and processor power supply [4]. These significant features place the FSBB converter one step ahead of the traditional DC-DC converters. For this reason, the FSBB converter topology received the attention of many researchers. On the other hand, unlike the traditional buck-boost converter topology in which the output voltage polarities are inverted, the FSBB converter offers an output voltage with non-inverted polarities. This feature is very useful in some applications where no isolation is needed between input and output. The bidirectional power flow capability of the FSBB converter makes it a good candidate in battery applications.

In addition to the FSBB converter topology [5], various buck-boost converter topologies such as auxiliary circuit based noninverting buck-boost converter [6], continuous-conduction mode noninverting buck-boost converter [7], input-parallel output-series buck-boost converter [8], digital noninverting-buck-boost converter [9], synchronous noninverting buck-boost

converter [10], auxiliary-component sharing based synchronous non-inverting buck-boost converter [11] are studied in the literature. However, among these buck-boost converters, the FSBB converter is the best one in terms of less passive component requirement, non-inverted output voltage polarities and bidirectional power flow capability [12]. It is possible to operate the FSBB as a traditional boost and buck converter by applying appropriate switching signals. Unlike the traditional buck-boost converter, each operation mode (buck mode and boost mode) is structured with separate switches. As such, the controller to be designed for the FSBB converter should be able to achieve the desired control objectives during the buck and boost operation modes. The most desired control objective in DC-DC converters is the load voltage regulation against load, input voltage and reference load voltage variations. In order to achieve this objective, the inductor current control is essential.

Various control approaches are developed for FSBB converters. In [13], a finite control set-model predictive control (FCS-MPC) method which selects the proper switching signals based on the evaluation of the cost function in the finite control set technique is proposed. The reference of the inductor current is produced by a PI regulator. In this method, the switching frequency is dependent on the operating point of the FSBB. In addition, an online weighting factor update method is essential in this control strategy. However, the controller performance is dependent on the model parameters since the MPC technique uses mathematical model of the FSBB converter. Another disadvantage of the FCS-MPC method is the variable switching frequency that is not preferred in a real-time application. The variable switching frequency exists due the use of finite control set structure. The dependency of the model parameters can be tackled by using the sliding mode control (SMC) method. In SMC methods, the pulse width modulation signals are easily generated by using either hysteresis modulation or traditional modulation methods depending on the sliding surface function formulation and SMC design. However, the determination of sliding gains in the sliding surface function is usually based on the trial-and-error approach. So far, there is no SMC method devoted for the FSBB converters.

In [14], the current mode control is achieved via proportional-integral (PI) control with the combination of smooth mode shifting. In this case, the operation mode of the FSBB converter is decided by using a special algorithm which

complicates the implementation. The control method in [15] is also based on MPC where the duty cycle is predicted and the pulse width modulation signals are produced depending on the inductor current slope. A predefined minimum duty cycle value is required to implement this method successfully. Also, the operation mode is determined by using the minimum duty cycle value. In [16], an improved single-mode control strategy is introduced which controls the output voltage only in boost mode. It is worthy remarking that such control is possible if the duty cycle of the buck stage is fixed while the duty cycle of the boost stage is controlled. In [12], [17] and [18], the control methods which are based on mode transition are also studied for the FSBB converters. Even though these mode transition methods can be combined with the control methods, the combination increases the implantation complexity of the controller.

In this paper, a passivity based control method is introduced for a FSBB converter. The control input equations are determined separately so as to obtain the duty cycle of buck and boost stages. The approximate values of damping gains are determined analytically which are useful in designing the converter for different operating points. While the load voltage (capacitor voltage) is controlled by a PI regulator, the passivity based control achieves the control of inductor current. The switching signals are produced by comparing the duty cycles with a triangular carrier. An important advantage of the proposed control approach is that it does not need any mode transition (or detection) algorithm which leads to simplicity compared with the existing control approaches.

## II. MODELING AND OPERATION PRINCIPLE

Fig. 1 depicts a four switch buck-boost DC-DC converter which contains four switching devices ( $S_1, S_2, S_3$  and  $S_4$ ). While  $S_1$  and  $S_2$  are connected on the same leg at the input side,  $S_3$  and  $S_4$  are connected on another leg at the output side of the converter. The midpoint of  $S_1$  and  $S_2$  are connected to the midpoint of  $S_3$  and  $S_4$  through an inductor ( $L$ ) whose resistance is denoted by  $R_L$ . The mathematical model of the converter can be written by considering the states of switching devices. Now, assuming that  $S_3$  is ON and  $S_4$  is OFF, one can write the following differential equations

$$\begin{aligned} \checkmark \text{ KVL} &\Rightarrow L \frac{di_L}{dt} = V_{in} u_1 - R_L i_L - V_C \\ \checkmark \text{ KCL} &\Rightarrow C \frac{dV_C}{dt} = i_L - \frac{V_C}{R} \end{aligned} \quad (2)$$

Similarly, assuming that  $S_3$  is OFF and  $S_4$  is ON, we can write the following equations

$$\begin{aligned} \checkmark L \frac{di_L}{dt} &= V_{in} u_1 - R_L i_L \\ C \frac{dV_C}{dt} &= -\frac{V_C}{R} \end{aligned} \quad (3)$$

$$\text{KVL: } i_L R_L + L \frac{di_L}{dt} = V_{in} u_1 \quad (4)$$

Now, combining (1)-(4) yields

$$L \frac{di_L}{dt} = V_{in} u_1 - R_L i_L - V_C (1-u_2) \quad (5)$$

$$C \frac{dV_C}{dt} = i_L (1-u_2) - \frac{V_C}{R} \quad (6)$$

modify: add one capacitance

$\text{if } S_3 \vee S_4 \text{ X}$

$\sum S_3 \times S_4 \text{ V}$

$\text{KVL}$

$\text{KCL}$

In equations (1)-(6),  $u_1$  and  $u_2$  denote the control inputs which are defined as

$$\begin{cases} 0 & \Rightarrow S_1 = \text{OFF}, \\ 1 & \Rightarrow S_1 = \text{ON}, \end{cases} \quad \begin{cases} S_2 = \text{ON} \\ S_2 = \text{OFF} \end{cases} \quad (7)$$

$$\begin{cases} 1 & \Rightarrow S_3 = \text{OFF}, \\ 0 & \Rightarrow S_3 = \text{ON}, \end{cases} \quad \begin{cases} S_4 = \text{ON} \\ S_4 = \text{OFF} \end{cases} \quad (8)$$

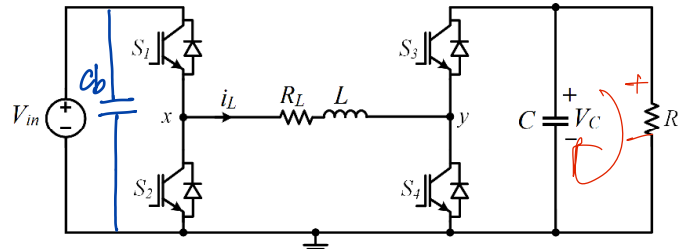


Fig. 1. Four switch buck-boost DC-DC converter.

The switching states and corresponding voltages are listed in Table I. Clearly, only one switch is turned ON in the same converter leg while the other switch should be turned OFF so as to avoid shoot through. The equivalent circuits corresponding to each switching state are depicted in Fig. 2. Fig. 2(a) shows state 1 where  $S_1$  and  $S_3$  are ON, while  $S_2$  and  $S_4$  are OFF. In this case, the input DC voltage source delivers energy to the load. Fig. 2(b) shows state 2 where  $S_1$  and  $S_4$  are ON, while  $S_2$  and  $S_3$  are OFF. It is evident that the inductor is charged by the input DC voltage source. In this operating mode, the capacitor is discharged through the load. Fig. 2(c) shows state 3 where  $S_2$  and  $S_3$  are ON, while  $S_1$  and  $S_4$  are OFF. It is obvious that the inductor is discharged through load. When the converter changes its operation between state 1 and state 3,  $S_3$  is always ON while  $S_1$  and  $S_2$  are switched complementarily of each other. In this stage, the converter operates in the buck mode since the circuit obtained from the combination of state 1 and state 3 is equivalent to the circuit of a buck converter [19]. On the other hand, the converter operates in the boost mode when its operation is changed between state 1 and state 2. In this case,  $S_1$  is always ON while  $S_3$  and  $S_4$  are switched complementarily of each other. It can be easily verified that the circuit obtained from combination of state 1 and state 2 is equivalent to the circuit of a boost converter [20]. When the converter changes its operation between state 2 and state 3, it operates in the buck-boost mode in which the value of load voltage is determined by the duty ratio of state 2 and state 3. Finally, Fig. 2(d) shows state 4 where  $S_2$  and  $S_4$  are ON, while  $S_1$  and  $S_3$  are OFF. In state 4, the inductor current is circulated within the converter through  $S_2$  and  $S_4$ .

TABLE I  
SWITCHING STATES AND VOLTAGES

State	$S_1$	$S_2$	$S_3$	$S_4$	$V_x$	$V_y$
1	ON	OFF	ON	OFF	$V_{in}$	$V_c$
2	ON	OFF	OFF	ON	$V_{in}$	0
3	OFF	ON	ON	OFF	0	$V_c$
4	OFF	ON	OFF	ON	0	0

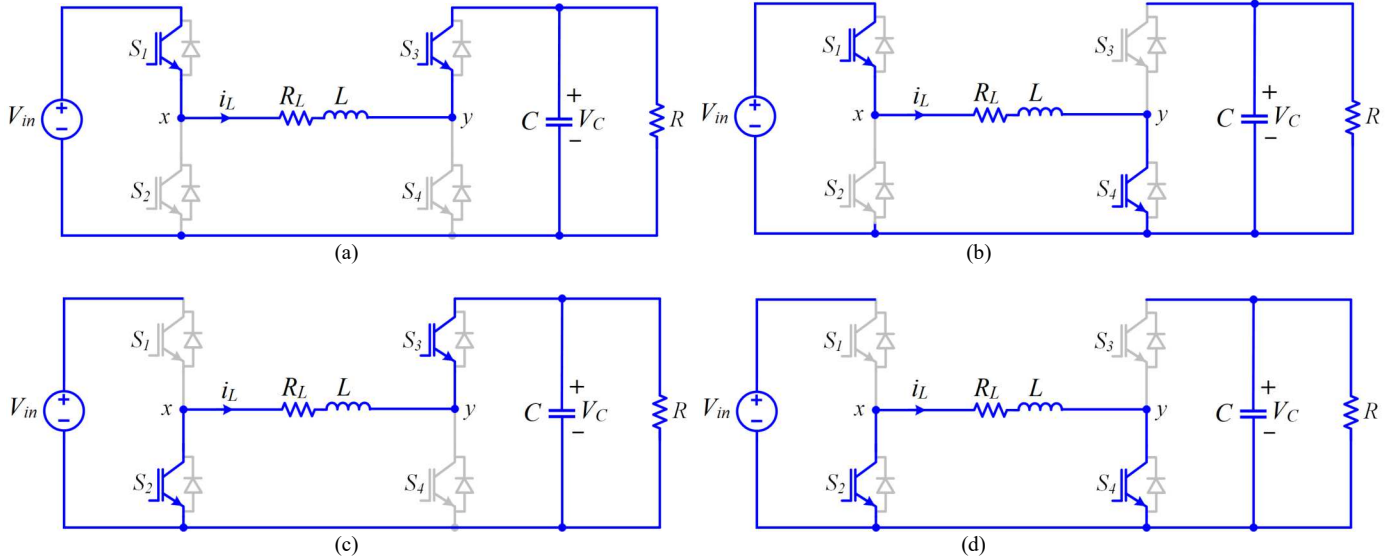


Fig. 2. Equivalent circuits corresponding to each switching state. (a) State 1, (b) State 2, (c) State 3, (d) State 4

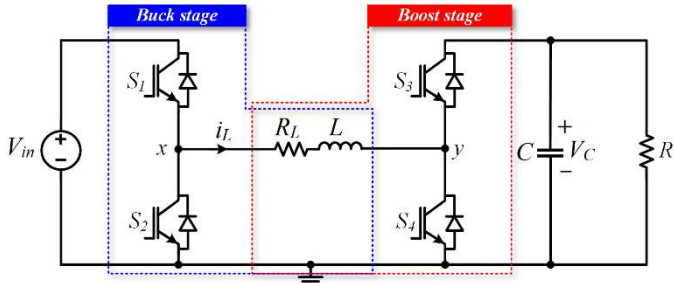


Fig. 3. Four switch buck-boost converter with buck and boost stages.

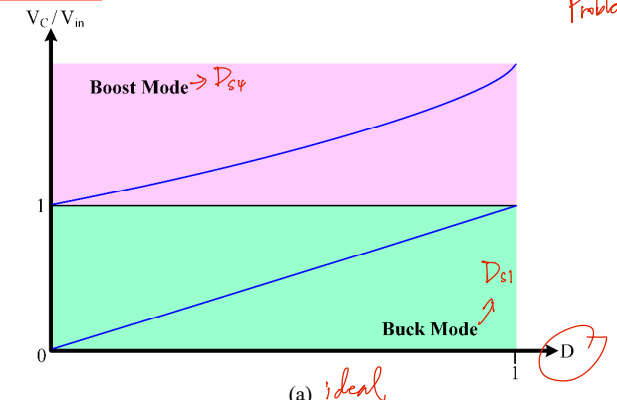
As explained before,  $S_1$  and  $S_2$  determine the buck operation and  $S_3$  and  $S_4$  determine the boost operation of the converter by sharing the inductor. Fig. 3 shows the FSBB converter with buck and boost stages shown explicitly. The relationship between  $V_{in}$  and  $V_C$  is written as [21]

$$\frac{V_C}{V_{in}} = \begin{cases} D, & V_{in} \geq V_C \Rightarrow D_{S1} \neq 0 \\ \frac{1}{1-D}, & V_{in} < V_C \Rightarrow D_{S4} \neq 1 \end{cases} \quad (9)$$

where  $V_C/V_{in}$  is the voltage gain and  $D$  represents the duty cycle of  $S_1$  when the converter operates in the buck mode or  $S_4$  when the converter operates in the boost mode. Even though  $D$  can take any value between 0 and 1 in the ideal case, the minimum and maximum values of  $D$  are different in a practical implementation in the real time. The main reason of this difference comes from the fact that the switching devices cannot be turned ON (or OFF) instantly. Also, the dead time used to avoid the shoot through limits the available duty cycle values.

For instance, substituting  $D=0$  into the first term in (9) yields a voltage gain equal to zero. Similarly, substituting  $D=1$  into the second term in (9) yields a voltage gain equal to infinity. Obviously, these voltage gain values are practically not possible. Fig. 4 shows the operation areas (buck and boost operation) of converter for the ideal and practical cases [13]. Fig. 4(a) depicts the operation areas of converter in the ideal case where  $D$  can

take 0 and 1 values which cause the voltage gain equal to 0 and  $\infty$ , respectively [13]. Fig. 4(b) depicts the operation areas for the practical case [13]. The inadmissible duty cycle values are inside the shaded areas. The area in which the voltage gain is close to 1 is called the dead zone. When the converter operates in this zone, the load voltage cannot be regulated properly. It is worthy to remark that the load voltage cannot be regulated properly when the converter changes its operation between buck and boost modes.



(a) ideal

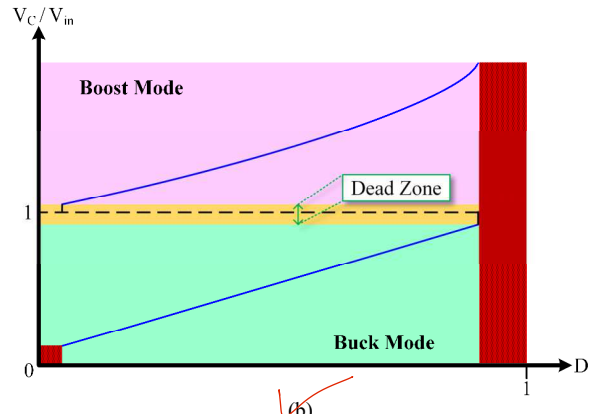


Fig. 4. Operation areas of four switch buck-boost converter. (a) Ideal case, (b) Practical case.

① 在此步驟考慮感抗

$$\left\{ \begin{array}{l} x_1 = i_L - i_L^* \\ x_2 = i_R - i_R^* \end{array} \right. \Rightarrow \left\{ \begin{array}{l} i_L = x_1 + i_L^* \\ i_R = x_2 + i_R^* \end{array} \right.$$

列出 KCL 和 KVL 方程

$$\left\{ \begin{array}{l} C \frac{dV_c}{dt} + i_R = i_L \\ i_R R = V_c \end{array} \right. \text{KCL} \Rightarrow \frac{dV_c}{dt} = \frac{di_R}{dt} \text{ (由常數)} \quad \Downarrow$$

$$\left\{ \begin{array}{l} L \frac{di_L}{dt} = V_{in} U_1 - R_L i_L - i_R R (1-U_2) \\ C \frac{di_R}{dt} \cdot R = i_L (1-U_2) - i_R \end{array} \right.$$

$$\textcircled{1} L \cdot \dot{x}_1 + L \frac{di^*}{dt} = V_{in} U_1 - R_L (x_1 + i_L^*) - (x_2 + i_R^*) R (1-U_2)$$

$$L \dot{x}_1 + R_L x_1 + x_2 R (1-U_2) = -L \frac{di^*}{dt} + V_{in} U_1 - R_L i_L^* - i_R^* R (1-U_2) + z_1 x_1$$

$$\textcircled{2} C \cdot \dot{x}_2 \cdot R + C \cdot \frac{di^*}{dt} \cdot R = x_1 (1-U_2) + i_L^* (1-U_2) - x_2 - i_R^*$$

$$C \dot{x}_2 \cdot R - x_1 (1-U_2) + x_2 = -C \frac{di^*}{dt} \cdot R + i_L^* (1-U_2) - i_R^* + z_2 x_2$$

$$\left\{ \begin{array}{l} U_2 = \frac{1}{i_L^*} \left( -i_L^* - C \cdot R \frac{di^*}{dt} - i_R^* + z_2 x_2 \right) \\ U_1 = \frac{1}{V_{in}} \left( L \frac{di_L^*}{dt} + R_L i_L^* + i_L^* R (1-U_2) - z_1 x_1 \right) \end{array} \right.$$

$$\text{恒定} \quad \left\{ \begin{array}{l} L \frac{di_L}{dt} = V_{in} U_1 - R_L i_L - V_c (1-U_2) \\ C \frac{dV_c}{dt} = i_L (1-U_2) - i_{out} \end{array} \right.$$

$$\left\{ \begin{array}{l} x_1 = i_L - i_L^* \\ x_2 = V_c - V_c^* \end{array} \right. \Rightarrow \left\{ \begin{array}{l} i_L = x_1 + i_L^* \\ V_c = x_2 + V_c^* \end{array} \right.$$

$$\textcircled{1} \quad \left\{ \begin{array}{l} L \cdot \dot{x}_1 + L \frac{di^*}{dt} = V_{in} U_1 - R_L \cdot (x_1 + i_L^*) - (x_2 + V_c^*) (1-U_2) \\ L \dot{x}_1 + R_L x_1 + x_2 (1-U_2) = V_{in} U_1 - R_L i_L^* - L \frac{di^*}{dt} - V_c^* (1-U_2) + z_2 x_2 \end{array} \right.$$

$$\textcircled{2} \quad C \cdot \dot{x}_2 + C \cdot \frac{dV_c^*}{dt} = (x_1 + i_L^*) (1-U_2) - i_{out}$$

$$C \cdot \dot{x}_2 - x_1 (1-U_2) = i_L^* (1-U_2) - i_{out} - C \frac{dV_c^*}{dt} + z_2 x_2$$

$$U_2 = \frac{1}{i_L^*} \left( i_L^* - i_{out} - C \frac{dV_c^*}{dt} + z_2 x_2 \right)$$

$$U_1 = \frac{1}{V_{in}} \left( R_L i_L^* + L \frac{di_L^*}{dt} + V_c^* (1-U_2) - z_1 x_1 \right)$$

② 考慮感抗和電容

$$\text{KVL} \quad \left\{ \begin{array}{l} L \cdot \frac{di_L}{dt} = V_{in} U_1 - R_L i_L - V_c (1-U_2) \\ C \cdot \frac{dV_c}{dt} = i_L (1-U_2) - i_{out} \end{array} \right.$$

$$\left\{ \begin{array}{l} i_L = x_1 + i_L^* \\ i_{out} = x_2 + i_{out}^* \end{array} \right. \quad \text{RHS}$$

$$\left\{ \begin{array}{l} i_L = x_1 + i_L^* \\ i_{out} = x_2 + i_{out}^* \end{array} \right.$$

$$\textcircled{1} \quad \left\{ \begin{array}{l} L \cdot \dot{x}_1 + L \frac{di^*}{dt} = V_{in} U_1 - R_L x_1 - R_L i_L^* - V_c (1-U_2) \\ L \dot{x}_1 + R_L x_1 = V_{in} U_1 - L \frac{di^*}{dt} - R_L i_L^* - V_c (1-U_2) + z_2 x_2 \end{array} \right.$$

$$\textcircled{2} \quad C \cdot \frac{dV_c}{dt} = (x_1 + i_L^*) (1-U_2) - (x_2 + i_{out}^*)$$

$$\left. \begin{array}{l} \dot{x}_2 + x_2 = -C \frac{dV_c}{dt} + i_L^* (1-U_2) - i_{out}^* \\ -x_1 (1-U_2) + x_2 = \end{array} \right. \quad \text{RHS } U_1, U_2$$

$$\left\{ \begin{array}{l} U_2 = \frac{1}{i_L^*} \left( i_L^* - C \frac{dV_c}{dt} - i_{out}^* + z_2 x_2 \right) \\ U_1 = \frac{1}{V_{in}} \left( L \frac{di^*}{dt} + R_L i_L^* + V_c (1-U_2) - z_1 x_1 \right) \end{array} \right.$$

Now, combining (1)-(4) yields

$$L \frac{di_L}{dt} = V_{in} u_1 - R_L i_L - V_C (1 - u_2) \quad (5)$$

$$C \frac{dV_C}{dt} = i_L (1 - u_2) - \frac{V_C}{R} \quad (6)$$

### III. PASSIVITY BASED CONTROL OF FSBB CONVERTER

#### A. Passivity Based Control Design

The control objectives in FSBB converter are the regulation of  $V_C$  and accurate  $i_L$  tracking under various scenarios such as variations in  $V_{in}$ ,  $R$  and  $V_C^*$ . In this study, a passivity based control approach is considered to achieve these control objectives. The state variables are defined as

$$x_1 = i_L - i_L^* \Rightarrow \text{误差} \quad (10)$$

$$x_2 = V_C - V_C^* \Rightarrow \text{误差} \quad (11)$$

Now, substituting  $i_L = x_1 + i_L^*$  and  $V_C = x_2 + V_C^*$  into (5) and (6), one can obtain the following equations

$$L \dot{x}_1 + R_L x_1 + x_2 (1 - u_2) = V_{in} u_1 - L \frac{di_L^*}{dt} - R_L i_L^* + V_C^* (u_2 - 1) \quad (12)$$

$$C \dot{x}_2 + x_1 (u_2 - 1) + \frac{x_2}{R} = i_L^* - i_L^* u_2 - C \frac{dV_C^*}{dt} - \frac{V_C^*}{R} \quad (13)$$

In equations (12) and (13), while the small signal components (i.e.:  $x_1$  and  $x_2$ ) are on the left hand side, the reference quantities (i.e.:  $i_L^*$  and  $V_C^*$ ) are on the right hand side. The passivity based controller is based on the damping injection which is added to both sides of (12) and (13) as follows [22]

$$L \dot{x}_1 + R_L x_1 + x_2 (1 - u_2) + \zeta_1 x_1 = V_{in} u_1 - L \frac{di_L^*}{dt} - R_L i_L^* + V_C^* (u_2 - 1) + \zeta_1 x_1 \quad (14)$$

$$C \dot{x}_2 + x_1 (u_2 - 1) + \frac{x_2}{R} + \zeta_2 x_2 = i_L^* - i_L^* u_2 - C \frac{dV_C^*}{dt} - \frac{V_C^*}{R} + \zeta_2 x_2 \quad (15)$$

In (14) and (15),  $\zeta_1$  and  $\zeta_2$  denote positive damping gains. Since the state variables are expected to converge to zero in the steady-state, then the left hand side of (14) and (15) can be equated to zero as follows  $\Rightarrow \zeta_1, \zeta_2 = 0$

$$0 = V_{in} u_1 - L \frac{di_L^*}{dt} - R_L i_L^* + V_C^* (u_2 - 1) + \zeta_1 x_1 \quad (16)$$

$$0 = i_L^* - i_L^* u_2 - C \frac{dV_C^*}{dt} - \frac{V_C^*}{R} + \zeta_2 x_2 \quad (17)$$

Now, solving for  $u_1$  and  $u_2$  yields

$$u_1 = \frac{1}{V_{in}} \left( L \frac{di_L^*}{dt} + R_L i_L^* + V_C^* (1 - u_2) - \zeta_1 x_1 \right) \quad (18)$$

$$u_2 = \frac{1}{i_L^*} \left( i_L^* - C \frac{dV_C^*}{dt} - \frac{V_C^*}{R} + \zeta_2 x_2 \right) \quad (19)$$

In (18) and (19),  $i_L^*$  can be generated by a proportional-integral (PI) regulator as follows

$$i_L^* = K_p (V_C^* - V_C) + K_i \int (V_C^* - V_C) dt \quad (20)$$

where  $K_p$  and  $K_i$  are the proportional and integral gains, respectively. It is clear that the control input  $u_1$  is dependent on the control input  $u_2$ .

PI 调节

若要调恒流

$$\begin{cases} X_1 = i_L^* - i_L \\ X_2 = V_C - V_C^* \end{cases}$$

#### B. Selection of Damping Gains

Now, substituting (19) into (6), one can obtain

$$C \frac{dV_C}{dt} - \frac{i_L^*}{i_L^*} C \frac{dV_C^*}{dt} + \frac{V_C}{R} - \frac{i_L^* V_C^*}{i_L^* R} - \frac{i_L^*}{i_L^*} \zeta_2 x_2 = 0 \quad (21)$$

Assuming that  $x_1 = 0$  (i.e.:  $i_L = i_L^*$ ), then (21) reduces to

$$\dot{x}_2 + \frac{(1 - R\zeta_2)}{RC} x_2 = 0 \quad (22)$$

The solution of (22) is given by

$$x_2 = x_2(0) e^{-At} \quad (23)$$

where  $x_2(0)$  is the initial point of  $x_2$  and  $A = \frac{1 - R\zeta_2}{RC}$ . It is

obvious that  $x_2$  converges to zero if  $\zeta_2 < \frac{1}{R}$  holds. On the other hand, substituting (18) into (5) yields

$$L \dot{x}_1 + R_L x_1 + \zeta_1 x_1 = (u_2 - 1) x_2 \quad (24)$$

Substituting (19) into (24) and assuming that  $x_2 = 0$  (i.e.:  $V_C = V_C^*$ ), one can obtain

$$L \dot{x}_1 + (R_L + \zeta_1) x_1 = 0 \quad (25)$$

The solution of (25) is given by

$$x_1 = x_1(0) e^{-Bt} \quad (26)$$

where  $x_1(0)$  is the initial point of  $x_1$  and  $B = \frac{R_L + \zeta_1}{L}$ . Since

$R_L > 0$  and  $\zeta_1 > 0$ ,  $x_1$  converges to zero at a rate determined by the time constant  $\frac{L}{R_L + \zeta_1}$ . Hence, the rate of convergence of

$x_1$  becomes faster if  $\zeta_1$  is increased. However, the value of  $\zeta_1$  should be selected such that  $u_1$  does not exceed 1. Although the equations (23) and (26) are obtained based on the assumptions that  $i_L = i_L^*$  and  $V_C = V_C^*$ , they are useful to select the approximate values of the damping gains  $\zeta_1$  and  $\zeta_2$ . The block diagram of the FSBB converter with passivity based control is depicted in Fig. 5.

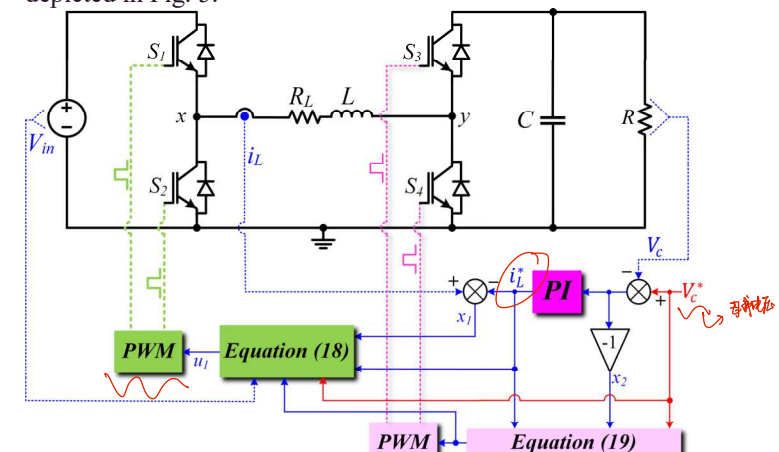


Fig. 5. Block diagram of the passivity based control method.

#### IV. SIMULATION RESULTS

The effectiveness of the proposed passivity-based control approach is studied through MATLAB/Simulink simulation studies where the system and control parameters shown in Table II are used.

TABLE II  
SYSTEM AND CONTROL PARAMETERS

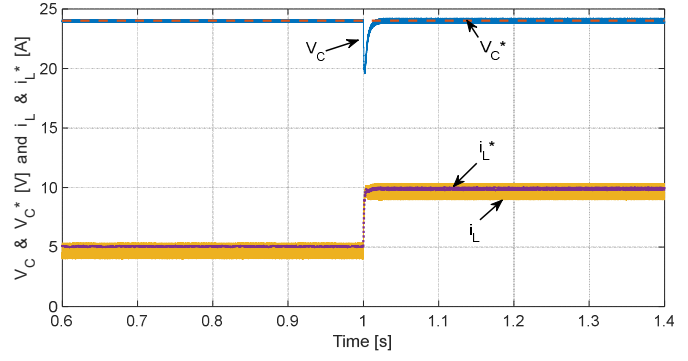
Parameters	Symbol	Value
DC input voltage	$V_{in}$	18V, 36V
Capacitor voltage reference	$V_C^*$	24V, 36V and 48V
Inductance	$L$	300μH
Resistance of inductor	$R_L$	0.04Ω
Capacitor	$C$	600μF
Resistive load	$R$	10Ω and 5Ω
PI gains	$K_p, K_i$	0.7, 200
Damping gains	$\zeta_1, \zeta_2$	6, 0.08
Switching frequency	$f_{sw}$	10kHz

Fig. 6(a) shows the dynamic responses of the capacitor voltage ( $V_C$ ), capacitor voltage reference ( $V_C^*$ ), inductor current ( $i_L$ ), and inductor current reference ( $i_L^*$ ) for a sudden load change from  $R=10\Omega$  to  $R=5\Omega$  while the converter is operated in the boost mode with  $V_{in}=18V$  and  $V_C^*=24V$ . It is evident that

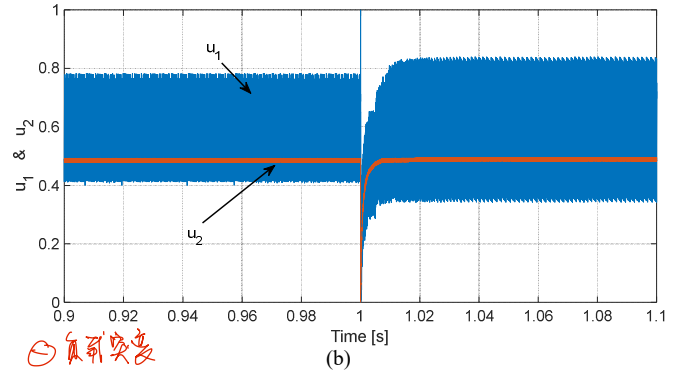
手写注释: NPI 稳定性  
跟踪精度  
响应速度  
 $V_C$  is regulated at 24V before and after the load change. Also,  $i_L$  tracks its new reference that is generated by the PI regulator in response to the load change. Fig. 6(b) shows the responses of control inputs  $u_1$  and  $u_2$ . While the average value of  $u_1$  is around 0.6, the average value of  $u_2$  is 0.5. It is worthy to note that these values are in good agreement with equations (18) and (19).

Fig. 7 shows the performance of passivity based control when the operation of converter is switched from buck mode to boost mode by changing. Fig. 7(a) shows the dynamic responses of  $V_C$  and  $i_L$  for a sudden change in  $V_{in}$  from 36V to 18V under  $R=10\Omega$  and  $V_C^*=24V$ . Before the change in  $V_{in}$ , the converter operates in the buck mode and  $V_C$  is regulated at 24V. After the sudden change in  $V_{in}$ , the converter operates in the boost mode and  $V_C$  exhibits a fast transient and settles down at 24V again. These results confirm the superiority of the proposed control method when the converter changes its operation mode. Fig. 7(b) shows the responses of  $u_1$  and  $u_2$  corresponding to the abrupt change in  $V_{in}$ . It is apparent that the values of  $u_1$  and  $u_2$  are changed after  $V_{in}$  is changed.

Fig. 8 shows the performance of the passivity based control for a variation in  $V_C^*$  from 24V to 48V. Initially, the converter operates in the buck mode with  $V_{in}=36V$  and  $V_C^*=24V$ .

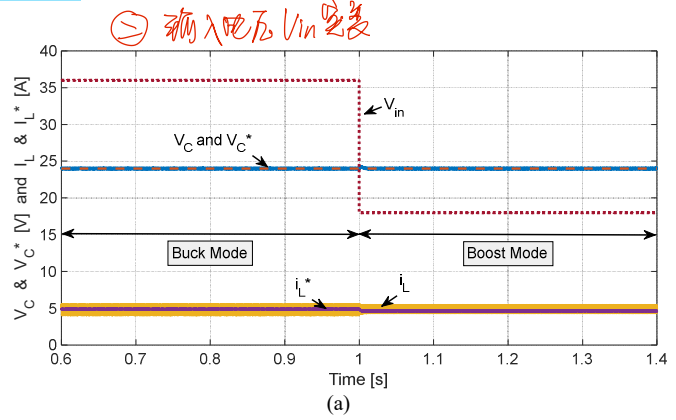


(a)

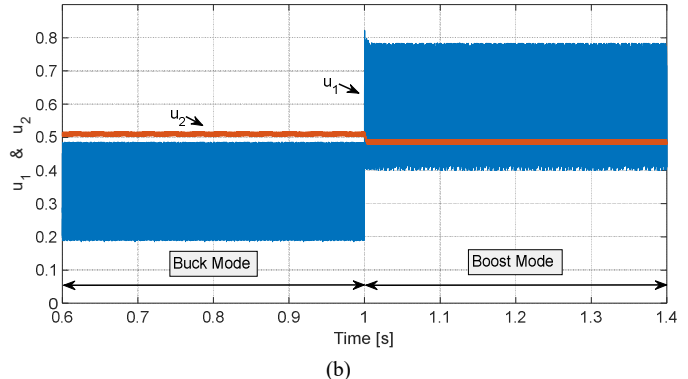


(b)

Fig. 6. (a) Dynamic performance of the controller for a sudden load change from  $10\Omega$  to  $5\Omega$  when the converter is operated in the boost mode, (b) Responses of  $u_1$  and  $u_2$ .



(a)



(b)

Fig. 7. Performance of the proposed control method when the converter switches from buck mode to boost mode under  $R=10\Omega$ .

$\Sigma$   $V_C$   $\Sigma$

It is apparent that  $V_C$  is regulated at 24V for  $V_C^* = 24V$ . When  $V_C^*$  is changed to 48V, the controller reacts to this change and forces  $V_C$  and  $i_L$  to track  $V_C^*$  and  $i_L^*$ , respectively. It should be mentioned that the operation mode of the converter is switched from buck mode to boost mode. In general, such operation mode transition results in undesired disturbances in  $V_C$  due to the dead zone shown in Fig. 4(b). However, as can be seen from Fig. 8,  $V_C$  is not distorted when the converter switches its operation mode.

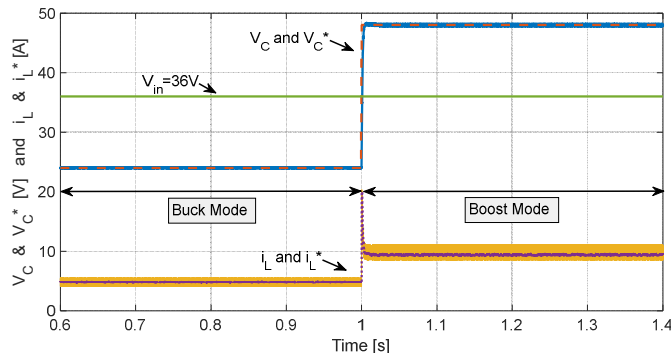


Fig. 8. Performance of the proposed control method when the converter switches from buck mode to boost mode by varying  $V_C^*$ .

## V. CONCLUSION

In this paper, a passivity based control method is introduced for a FSBB converter. Unlike most of the existing methods, the proposed control method removes the mode detection algorithm requirement. The capacitor voltage is not distorted when the converter changes its operation mode. The simulation results reveal that the proposed control method can regulate the capacitor voltage and inductor current to their references in buck and boost modes. These results verify that the proposed control method can be a good choice for the FSBB converters.

## ACKNOWLEDGMENT

This publication was made possible by NPRP12S-0214-190083 from the Qatar National Research Fund (a member of Qatar Foundation). The statements made herein are solely the responsibility of the authors.

## REFERENCES

- [1] X. Ren, Z. Tang, X. Ruan, J. Wei, and G. Hua, "Four switch buck-boost converter for telecom DC-DC power supply applications," *Conf. Proc. - IEEE Appl. Power Electron. Conf. Expo. - APEC*, pp. 1527–1530, 2008, Austin, TX, USA.
- [2] M. Orellana, S. Petibon, B. Estibals and C. Alonso, "Four switch buck-boost converter for photovoltaic DC-DC power applications", *IECON 2010 - 36th Annual Conference on IEEE Industrial Electronics Society*, pp. 469-474, 2010, Glendale, AZ, USA.
- [3] Y. Qin, S. Li, and S. Y. Hui, "Topology-transition control for wide-input-voltage-range efficiency improvement and fast current regulation in automotive LED applications," *IEEE Trans. Ind. Electron.*, vol. 64, no. 7, pp. 5883–5893, 2017.
- [4] T. Urkin and M. M. Peretz, "Digital CPM controller for a non-inverting buck-boost converter with unified hardware for steady-state and optimized transient conditions," *IEEE Trans. Power Electron.*, vol. 35, no. 8, pp. 8794–8804, 2020.
- [5] C. Chang and C. Wei, "Single-inductor four-switch non-Inverting buck-boost DC-DC converter," *Proceedings of 2011 International Symposium on VLSI Design, Automation and Test*, pp. 20–23, 2011, Hsinchu, Taiwan.
- [6] Y. Zhang, X. F. Cheng, and C. Yin, "A soft-switching synchronous rectification noninverting buck-boost converter with a new auxiliary circuit," *IEEE Trans. Ind. Electron.*, vol. 68, no. 9, pp. 7931–7937, 2021.
- [7] P. J. Liu and C. W. Chang, "CCM noninverting buck-boost converter with fast duty-cycle calculation control for line transient improvement," *IEEE Trans. Power Electron.*, vol. 33, no. 6, pp. 5097–5107, 2018.
- [8] N. Rana and S. Banerjee, "Development of an improved input-parallel output-series buck-boost converter and its closed-loop control," *IEEE Trans. Ind. Electron.*, vol. 67, no. 8, pp. 6428–6438, 2020.
- [9] Y. Tsai, Y. Tsai, C. Tsai, and C. Tsai, "Digital noninverting-buck-boost converter with enhanced duty-cycle-overlap control," *IEEE Transactions on Circuits and Systems II: Express Briefs*, vol. 64, no. 1, pp. 41–45, Jan. 2017.
- [10] C. Restrepo, T. Konjedic, J. Calvente, and R. Giral, "Hysteretic transition method for avoiding the dead-zone effect and subharmonics in a noninverting buck-boost converter," *IEEE Trans. Power Electron.*, vol. 30, no. 6, pp. 3418–3430, 2015.
- [11] L. Cong, J. Liu, and H. Lee, "A high-efficiency low-profile zero-voltage transition synchronous non-inverting buck-boost converter with auxiliary-component sharing," *IEEE Trans. Circuits Syst. I Regul. Pap.*, vol. 66, no. 1, pp. 438–449, 2019.
- [12] P. C. Huang, W. Q. Wu, H. H. Ho, and K. H. Chen, "High efficiency and smooth transition buck-boost converter for extending battery life in portable devices," *2009 IEEE Energy Convers. Congr. Expo. ECCE 2009*, vol. 2, no. 2, pp. 2869–2872, 2009.
- [13] X. Li, Y. Liu and Y. Xue, "Four-switch buck-boost converter based on model predictive control with smooth mode transition capability," *IEEE Trans. Ind. Electron.*, vol. 68, no. 10, pp. 9058–9069, Oct. 2021.
- [14] Q. Ullah, X. Wu and U. Saleem, "Current controlled robust four-switch buck-boost DC-DC converter," *2021 International Conference on Computing, Electronic and Electrical Engineering (ICE Cube)*, pp. 1-6, 2021.
- [15] Y. Bai, S. Hu, Z. Yang, Z. Zhu, and Y. Zhang, "Model predictive control for four-switch buck-boost converter based on tuning-free cost function with smooth mode transition," *IEEE J. Emerg. Sel. Top. Power Electron.*, vol. 6777, no. c, pp. 1–1, 2021.
- [16] Y. Wang, J. Lan, X. Huang, T. Fang, X. Ruan, and M. Dong, "An improved single-mode control strategy based on four-switch buck-boost converter," *Conf. Proc. - IEEE Appl. Power Electron. Conf. Expo. - APEC*, vol. 2020-March, pp. 320–325, 2020.
- [17] Y. M. Chen, Y. L. Chen, and C. W. Chen, "Progressive smooth transition for four-switch buck-boost converter in photovoltaic applications," *IEEE Energy Convers. Congr. Expo. Energy Convers. Innov. a Clean Energy Futur. ECCE 2011, Proc.*, pp. 3620–3625, 2011.
- [18] M. F. Ceci and M. B. D'Amico, "An alternative strategy for reducing mode transitions in a four-switch buck-boost converter," *Proc. - IEEE Int. Symp. Circuits Syst.*, pp. 1920–1923, 2011.
- [19] H. Komurcugil, "Adaptive terminal sliding-mode control strategy for DC-DC buck converters," *ISA Transactions*, vol. 51, no. 6, pp. 673–681, November 2012.
- [20] H. Komurcugil, "A PI-type self-tuning fuzzy logic controller for DC-DC boost converters," in *Proc. of the 30th Annual Conference of the IEEE Industrial Electronics Society (IECON)*, pp. 209-214, 2004, Busan, Korea.
- [21] L. Callegaro, M. Ciobotaru, D. J. Pagano, E. Turano, and J. E. Fletcher, "A simple smooth transition technique for the noninverting buck-boost converter," *IEEE Trans. Power Electron.*, vol. 33, no. 6, pp. 4906–4915, Jun. 2018.
- [22] H. Komurcugil, S. Bayhan, and M. Malinowski, "Passivity-based control strategy with improved robustness for single-phase three-level T-type rectifiers," *IEEE Access*, vol. 9, pp. 59336–59344, 2021.